Received: 12 October 2018 | Revised: 7 January 2019 | Accepted: 15 January 2019

DOI: 10.1111/cas.13950

ORIGINAL ARTICLE

WILEY Cancer Science

LncRNA MIR22HG inhibits growth, migration and invasion through regulating the miR-10a-5p/NCOR2 axis in hepatocellular carcinoma cells

Yangjun Wu | Yuqiang Zhou | Lin Huan | Linguo Xu | Mengting Shen | Shenglin Huang | Linhui Liang

Fudan University Shanghai Cancer Center and Institutes of Biomedical Sciences, Shanghai Medical College, Fudan University, Shanghai, China

Correspondence
Linhui Liang, Fudan University Shanghai Cancer Center and Institutes of Biomedical Sciences, Shanghai Medical College, Fudan University, Shanghai, China.
Email: lianglinhui@fudan.edu.cn

Funding information
National Natural Science Foundation of China, Grant/Award Number: 81672366

Despite the rapidly identified numbers of lncRNA in humans, exploration of the molecular mechanisms of lncRNA is lagging, because the molecular mechanisms of lncRNA can be various and complex in different conditions. In this study, we found a new molecular mechanism for a versatile molecule, MIR22HG. MIR22HG is an lncRNA that contributes to the initiation and progression of many human cancers, including hepatocellular carcinoma (HCC). We report that MIR22HG was downregulated in 120 HCC samples compared with adjacent nontumor liver tissues. More interestingly, decreased expression of MIR22HG in HCC could predict poor prognosis of HCC patients. Knockdown of MIR22HG promoted the growth, migration and invasion of HCC cells. In exploring the molecular mechanism of MIR22HG, we found that MIR22HG functioned as a tumor suppressor in hepatocellular carcinomas, in part through serving as a competing endogenous RNA to modulate the miRNA-10a-5p level. Moreover, NCOR2 was verified to act as the downstream target gene of MIR22HG/miR-10a-5p. In addition, the MIR22HG/miRNA-10a-5p/NCOR2 axis inhibited the activation of the Wnt/β-catenin pathway. Together, our results demonstrated that MIR22HG inhibited HCC progression in part through the miR-10a-5p/NCOR2 signaling axis and might act as a new prognostic biomarker for HCC patients.

KEYWORDS
hepatocellular carcinoma, LncRNA, miR-10a-5p, MIR22HG, NCOR2

1 | INTRODUCTION

Hepatocellular carcinoma (HCC) is the most common type of liver cancer and was the fourth leading cause of cancer death worldwide in 2018.[1,2] Liver transplantation and surgical resection may provide the opportunity for a cure only when patients are at an early stage. Even after surgical resection, the 5-year survival rate of HCC patients remains poor, owing to high rates of metastasis and recurrence.[3] Thus, it is critical to explore the molecular mechanisms underlying HCC progression and to identify novel targets for effective intervention.

Yangjun Wu and Yuqiang Zhou contributed equally to this work.

Long noncoding RNA (lncRNA) are transcripts longer than 200 nucleotides and do not have any apparent protein-coding poteintial.[4] Accumulating evidence shows that lncRNA play an important role in various physiological and pathological processes.[5] The mechanisms of lncRNA function have been shown to be multifactorial and largely dependent on their intracellular location. One molecular mechanism of the lncRNA enriched in the cytoplasm is participating in post–transcriptional regulation by acting as miRNA sponges.[6-8]

LncRNA MIR22HG, which is mostly located in cytoplasm, is frequently deleted or hypermethylated, and commonly shows loss of heterozygosity in HCC.[9] MIR22HG has previously been demonstrated to be downregulated in hepatocellular carcinoma.[10] MIR22HG repressed hepatocellular carcinoma cell invasion by deriving miR-22 to target HMGB1 and binding with human antigen R (HuR).[9] Su et al[11] revealed that MIR22HG could inhibit cell survival signaling via oncogenes YBX1, MET and p21 in lung cancer. Cui et al[12] showed that MIR22HG negatively regulated miR-141-3p to upregulate DAPK1 expression and inhibited endometrial carcinoma cell proliferation. It is obvious that MIR22HG exerts its function through different mechanisms depending on the context diversity. In the present study, we demonstrate that MIR22HG can inhibit HCC cell growth, migration and invasion through regulating the miR10a-5p/NCOR2 axis, which might provide a new therapeutic target for HCC treatment.

2 | MATERIALS AND METHODS

2.1 | Clinical specimens

A total of 120 liver cancer tissues and pair-matched adjacent nontumorous tissues were obtained from the Liver Cancer Institute of Zhongshan Hospital. A total of 38 pairs of human primary HCC and matched adjacent noncancerous liver tissues were collected from the Qi Dong Liver Cancer Institute/Hospital, Qi Dong, China. All human materials were obtained with informed consent. The study was approved by the Ethical Review Committee of the World Health Organization of the Collaborating Center for Research in Human Production and authorized by the Shanghai Municipal Government.

2.2 | Cell culture

HEK293T, Huh7, HepG2-C3A, SK-Hep-1 and MHCCLM3 cells were cultured at 37°C in a humidified incubator with 5% CO_2 in DMEM supplemented with 10% FBS, 100 U/mL penicillin and 100 μg/mL streptomycin.

2.3 | 5′ and 3′ RACE assay

5′ and 3′ RACE were used to determine the transcriptional initiation and termination sites of MIR22HG with a SMARTer RACE cDNA Amplification Kit (Clontech, CA, USA) as per the manufacturer's instructions. The sequences for the gene-specific PCR primers used for 5′ and 3′ RACE analysis are given in Table S1.

2.4 | Northern blot

We used a NorthernMax Kit from Ambion (Thermo Fisher Scientific, Carlsbad, CA, USA) and a DIG Northern Starter Kit (Roche, Indianapolis, IN, USA) with Digoxin-labeled RNA probes to detect MIR22HG in MHCCLM3 cells. The PCR primers of the probes of MIR22HG are listed in Table S1.

2.5 | Subcellular fractionation

The PARIS Kit (Life Technologies, MA, USA) was used to isolate the nuclear and cytoplasmic fractions. β-actin was used as the cytoplasmic endogenous control. U2 small nuclear RNA was used as the nuclear endogenous control.

2.6 | RNA extraction and quantitative RT-PCR

Total RNA was isolated from patient tissues and cultured cells using TRIzol Reagent (Invitrogen, Carlsbad, CA, USA) as per the manufacturer's instructions. Total RNA (500 ng) was reverse transcribed to high-quality cDNA with a PrimeScript Reverse Transcriptase Kit (Takara, Dalian, China). Then MIR22HG and miR10a-5p expression were determined by PCR with a SYBR Green PCR Kit (Takara) and a Bulge-Loop TM miRNA qRT-PCR Starter Kit (Applied RiboBio Biotechnology, Guangzhou, China), respectively. U6 was used to normalize the expression of miR10a-5p, and β-actin was used to normalize the expression of MIR22HG and NCOR2 mRNA. The primer sequences used are shown in Table S1.

2.7 | Lentivirus production and cell transfection

Negative control (NC), miR10a-5p mimics, miR10a-5p inhibitor, si-NC, si-MIR22HG and si-NCOR2 were all obtained from RiboBio. To construct stable cell lines, shRNA were designed and inserted into the Lenti-guide vector by Addgene (#52963). The human MIR22HG sequence was cloned from MHCCLM3 cell cDNA and cloned into the BamHI and EcoRI sites of the lentivirus expression vector pCDH-CMV-MCS-EF1-Puro (catalog number CD510B-1; System Bioscience, Palo Alto, CA, USA) to generate pCDH-MIR22HG. The NCOR2 expression vectors were constructed by inserting the respective open-reading frame sequences into the pCDH vector to generate pCDH-NCOR2. A transfection assay was done using Lipofectamine 2000 (Invitrogen) according to the manufacturer's protocol at approximately 50%-70% cell confluence.

2.8 | Cell Counting Kit-8 and colony formation assays

For the Cell Counting Kit-8 (CCK-8) assays, 24 hours after transfection, tumor cells were seeded into 96-well plates and successively cultured for 5 days to detect liver cancer cell proliferation. To each well we added with 10 μL Cell Counting Kit-8 (CCK-8) solution (Dojindo, Tokyo, Japan). After incubation for 2 hours, the absorbance

was measured at a wavelength of 450 nm. For the colony formation assay, tumor cells (1000 cells per well) were seeded into 6-well plates 48 hours after transfection. After 10 days of incubation, the cells were fixed in methanol and stained with .5% crystal violet for 15 minutes. The colonies were counted using Quantity One software (Bio-Rad, Hercules, CA, USA).

2.9 | Cell migration, invasion and wound healing assays

For invasion assays, Millicell chambers were coated with 30 μg of Matrigel (BD Biosciences, Franklin Lakes, NJ, USA). The migration assay was conducted similarly, without coating the chambers with Matrigel. Cells (1×10^5) were added to the chambers in serum-free medium. We added 500 μL DMEM containing 10% FBS to the lower chambers. After 24 or 48 hours incubation at 5% CO_2, the chambers were fixed with methanol and stained with .5% crystal violet for 15 minutes. Cells moving to the lower membrane were counted in 5 random fields. For wound healing assays, cells were placed into 6-well plates and cultured until 100% confluence. An artificial scratch was created using a 200-μL pipette tip. At 0, 24 and 48 hours after culturing in serum-free medium, wound closure images were captured in the same field under magnification. Cell healing rates were calculated by the fraction of cell coverage across the line. These experiments were performed in triplicate and repeated 3 times.

2.10 | Luciferase reporter and TOP/FOP reporter assays

Fragments of MIR22HG or NCOR2 3′UTR containing miR10a-5p binding sites were amplified by PCR and inserted into the psiCHECK-2 vector (Promega, Madison, WI, USA), designated as MIR22HG -WT and NCOR2-3′UTR-WT. The mutant (MUT) fragment of MIR22HG and the mutant (MUT) 3′-UTR fragment of NCOR2 with miR10a-5p binding site were cloned into a the psiCHECK-2 vector, respectively. HEK293T cells were co-transfected with WT (or MUT) reporter plasmid and an NC mimic, miR10a-5p mimic, NC inhibitor or miR10a-5p inhibitor for 48 hours. Then, luciferase activity was evaluated using the Luciferase Reporter Assay System (Promega). For the TOP/FOP reporter assay, cells were co-transfected with the Wnt/β-catenin signaling reporter TOP/FOP (Addgene, Cambridge, MA, USA), along with MIR22HG knockdown or overexpression vector, and/or siNCOR2 or the pCDH-NCOR2 plasmid. At 48 hours post–transfection, HEK-293T cells were lysed and luciferase activity was detected as previously described. HEK-293T cells treated with 20 mmol/L LiCl for 12 hours were used as a positive control.

2.11 | RNA immunoprecipitation assays

RNA immunoprecipitation (RIP) assays were used to investigate the potential endogenous interaction between MIR22HG and miR10a-5p using a Magna RIP RNA-Binding Protein Immunoprecipitation Kit (Millipore) as per the manufacturer's instructions. RNA was extracted using the Total RNA Isolation Kit (Invitrogen, Carlsbad, CA, USA), and quantitative RT-PCR (qRT-PCR) was performed as described above. The primary antibodies against Ago-2 and IgG were obtained from Abcam (Cambridge, MA, USA).

2.12 | Western blot analysis

After transfection for 48 hours, proteins were collected from cells using RIPA Buffer (Beyotime Biotechnology, Shanghai, China) containing proteinase and phosphatase inhibitors. The protein concentrations were determined using the BCA method (Pierce, Thermo Fisher Scientific Inc., Rockford, IL, USA). Equal amounts of proteins obtained from different kinds of cell lysates were separated by SDS-PAGE and transferred to PVDF membranes (Immobilon-P membrane, Millipore, MA, USA). After blocking with BSA, the membranes were incubated with primary antibodies and the corresponding secondary antibodies. Protein complex was visualized with Western Lightning Chemiluminescence Reagent Plus (Pierce). The primary antibodies used in this assay included E-cadherin, vimentin, N-cadherin, β-catenin, NCOR2 (Proteintech, Chicago, IL, USA), β-actin (Sigma), smad2, smad3 and slug (Cell Signaling Technology, Danvers, MA, USA). HRP-conjugated goat anti–rabbit or anti–mouse IgG antibody (Proteintech, Chicago, USA) was used as the secondary antibody.

2.13 | Statistical analysis

Statistical analyses were performed using IBM SPSS Statistics V19 package (Armonk, NY, USA). Data were presented as the mean ± SEM from multiple samples. The Student's *t* test or one-way ANOVA were used to evaluate the differences between different groups. Correlations between MIR22HG and NCOR2 or miR10a-5p were analyzed by Pearson rank correlation. Survival was calculated using the Kaplan-Meier method and analyzed using the log-rank test. $P < .05$ was considered statistically significant.

3 | RESULTS

3.1 | MIR22HG is significantly downregulated in hepatocellular carcinoma and low MIR22HG expression predicts poor prognosis

To explore the role of MIR22HG in HCC development, we first investigated the expression of MIR22HG in 120-pair HCC specimens (Figure 1A). We found that MIR22HG is distinctly downregulated in HCC specimens compared with adjacent nontumor liver tissues (Figure 1B). To investigate the clinical significance of MIR22HG expression in HCC, we analyzed the relationship between clinicopathologic features and MIR22HG expression levels in HCC cases. The MIR22HG level was negatively correlated with the level of AFP ($P = .012$) (Table 1). Importantly, downregulation of MIR22HG expression was associated with tumor thrombus ($P = .05$; Table 1). Furthermore, patients with lower MIR22HG level exhibited shorter overall survival (OS) ($P = .045$) and worse disease-free survival than

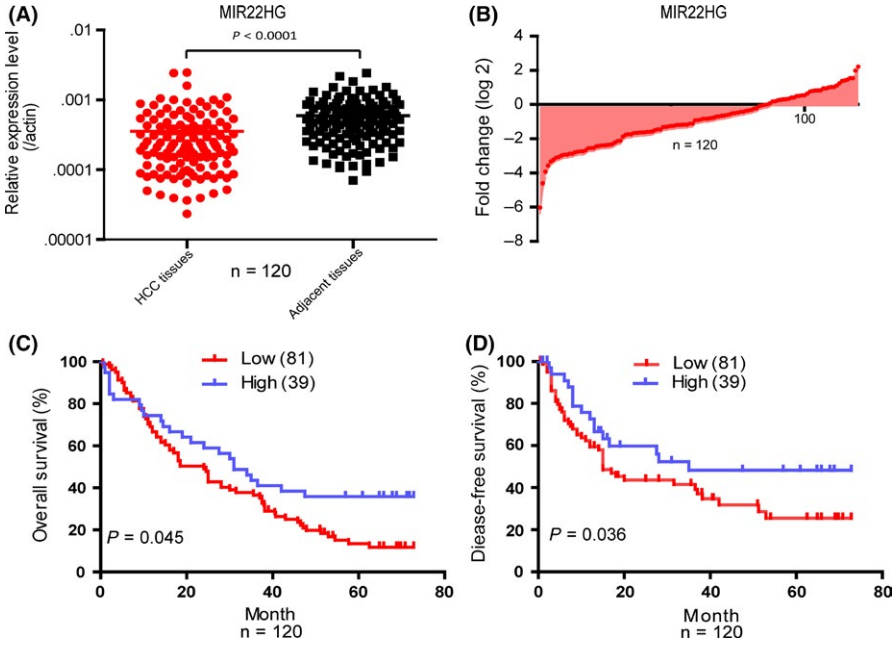

FIGURE 1 MIR22HG expression is downregulated in hepatocellular carcinoma (HCC) and predicts poor prognosis of patients with HCC. A, Quantitative PCR was used to detect MIR22HG mRNA expression in the adjacent nontumor liver tissue (n = 120) and HCC tissue (n = 120). Representative pictures of MIR22HG expression in HCC are shown. B, MIR22HG expression is downregulated in HCC. Kaplan-Meier plot of overall (C) and disease-free (D) survival of patients with HCC, stratified by MIR22HG expression

those with higher MIR22HG level (Figure 1C, D). These findings suggest that MIR22HG might play a critical role in HCC progression and could be a valuable biomarker for HCC patients.

MIR22HG has 4 annotated transcripts in the National Center for Biotechnology Information database (NCBI) (Figure S1A). The 4 transcripts were all predicted to be ncRNA with low coding potential by the Coding-Potential Assessment Tool (CPAT) and the Coding Potential Calculator (CPC; Figure S1B). The dominant MIR22HG transcript with 2378 nucleotides was identified by the 5′ and 3′ RACE assays and northern blot assays in MHCCLM3 cells (Figure S1C-E). We then detected MIR22HG expression level in 8 HCC cell lines by performing qRT-PCR analysis and found that the expression of MIR22HG was decreased along with ability of HCC cells to metastasize (Figure S1F). Next, we confirmed that approximately 85% of MIR22HG distribute in the cytoplasm (Figure S1G).

3.2 | MIR22HG inhibited hepatocellular carcinoma cell growth, migration and invasion

Next, to investigate the potential biological function of MIR22HG, we stably silenced MIR22HG in HepG2-C3A and MHCCLM3 cells (Figure 2A). CCK8 assays showed that downregulation of MIR22HG significantly promoted liver cancer cell growth (Figure 2B), and colony formation assays were consistent with this result (Figure 2C). Moreover, transwell assays indicated that knockdown of MIR22HG promoted the migration and invasion of cells compared with the control (Figure 2D). Wound healing assays showed that downregulation of MIR22HG promoted cell migration in HepG2-C3A and MHCCLM3 cells (Figure 2E).

Next, we constructed pCDH-MIR22HG expression plasmid and transfected it into Huh7 and SK-Hep-1 cells (Figure 3A). CCK8 assays showed that MIR22HG overexpression significantly decreased Huh7 and SK-Hep-1 cell growth (Figure 3B). The same results were obtained in colony formation assays (Figure 3C). Simultaneously, transwell assays and wound healing assays were used to evaluate cell migration and invasion following MIR22HG overexpression. As the results show, MIR22HG overexpression significantly suppressed the migration and invasion of Huh7 and SK-Hep-1 cells (Figure 3D, E). Taken together, MIR22HG acts as a tumor suppressor in liver cancer cells.

3.3 | MIR22HG directly interacts with miR-10a-5p

To further uncover the molecular mechanism by which MIR22HG exerts its biological function in HCC, we analyzed the microRNA (miRNA) binding sites on MIR22HG using the TargetScan algorithm. At the same time, we analyzed the correlation between MIR22HG with the miRNA candidates. Finally, 13 candidate miRNA were selected following this analytical strategy (Figure S2A). To explore the potential interaction of candidate miRNA and MIR22HG, we transfected these 13 miRNA mimics with psicheck2-MIR22HG plasmids into HEK-293T cells, respectively. We found that miR10a-5p mimic markedly altered the luciferase activity of the construct containing MIR22HG transcript (Figure 4A). Ago-2 RIP assays showed that MIR22HG and miR10a-5p could simultaneously be pulled down from the Ago-2 complex, which is a key component of the RNA-induced silencing complex (RISC) (Figure 4B). To investigate the interaction between MIR22HG and miR10a-5p, we performed several experiments. First, we evaluated the expression of MIR22HG and miR10a-5p in 38 pairs of HCC tissues and found that miR10a-5p expression was inversely correlated with MIR22HG expression in 38 pairs of HCC tissues ($r = -.365$, $P = .183$; Figure S2B). Second, we constructed luciferase reporter vectors containing either wild-type

TABLE 1 Clinical parameters of the patients with hepatocellular carcinoma (HCC) who were included in this study

	P-value	Low MIR22HG Case number	High MIR22HG Case number
Age			
>50	.104	37	24
≤50		44	15
Gender			
Male	.926	68	33
Female		13	6
HBsAg			
Negative	.368	15	10
Positive		66	29
HBcAb			
Negative	.156	5	6
Positive		76	33
Tumor size (cm)			
≤5 cm	.396	39	22
>5cm		42	17
AFP (ng/mL)			
≤200	.012	19	18
>200		62	21
Differentiation grade			
I/II	.068	57	34
III/IV		22	5
TNM			
Early stage	.402	37	21
Late stage		44	18
Tumor thrombus			
0	.05	41	27
≥1		40	12
Tumor number			
1	.33	70	31
≥2		11	8

(WT) or mutated (MUT) miR10a-5p binding site in MIR22HG (Figure 4C). The results of dual-luciferase reporter assays revealed that miR10a-5p mimic repressed the luciferase activity of the WT-MIR22HG reporter vector but had no effect on the MUT-MIR22HG vector (Figure 4D). Consistent with these results, when miR10a-5p inhibitor was transfected with these constructs into HEK-293T cells, luciferase reporter assays indicated that miR10a-5p inhibitor could induce the luciferase activity of WT-MIR22HG reporter vector but not MUT-MIR22HG vector. Meanwhile, qRT-PCR results indicated that overexpression of MIR22HG significantly reduced the miR10a-5p expression in SK-Hep-1 cells, while silencing MIR22HG increased miR10a-5p expression in MHCCLM3 cells (Figure 4E). These results indicate that MIR22HG could directly bind to miR10a-5p and affect its expression.

3.4 | MIR22HG acts as a competing endogenous RNA and regulates miR10a-5p downstream target NCOR2 by competitively binding to miR10a-5p

To elucidate the molecular mechanism underlying miR10a-5p exerting its effects on HCC cells, we searched for candidate downstream targets of miR10a-5p using combined analyzing bioinformatics tools (miRTarBase, miRbase and miRDB) (Figure S2C) and 13 candidates were selected. qRT-PCR analysis showed that MIR22HG knockdown decreased NCOR2 while MIR22HG overexpression upregulated NCOR2 (Figure S2D, E). According to predictions from TargetScan, we found that there was a potential binding site of miR10a-5p in the 3′UTR of NCOR2 and constructed a luciferase reporter vector containing either wild or mutant NCOR2 3′-UTR (Figure 4F). As shown in Figure 4G, miR10a-5p mimic significantly suppressed the activity of NCOR2-wild-type reporter, while miR10a-5p inhibitor significantly increased the activity of NCOR2-wild-type reporter. However, neither miR10a-5p mimic nor miR10a-5p inhibitor have any effect on the luciferase activity of vector containing mutant miR10a-5p binding site (Figure 4G). Moreover, the NCOR2 transcript level was negatively correlated with the miR10a-5p expression level ($P = .132$, $r = -.252$) (Figure S2F). Western blot analysis showed that silenced MIR22HG decreased NCOR2 protein while MIR22HG overexpression upregulated NCOR2 protein, and miR10a-5p transfection could reverse the effect of MIR22HG on NCOR2 protein (Figure 4H). Importantly, Pearson's correlation analysis showed that NCOR2 mRNA was positively correlated with MIR22HG in HCC tissues ($P < .0001$, $r = .678$; Figure 4I). In summary, MIR22HG might positively regulate NCOR2 expression by competitively binding to miR10a-5p.

3.5 | MIR22HG inhibits hepatocellular carcinoma cell growth, invasion and metastasis through targeting the miR10a-5p/NCOR2 axis

Many reports have indicated that miR10a-5p acts as an oncogene during cancer progression,[13–17] but the role of miR10a-5p in HCC remains unclear. Here, we found that miR10a-5p could promote the growth, migration and invasion of liver cancer cells (Figure 5A-C). Next, we investigated the functional interaction of MIR22HG and miR10a-5p. As shown in Figure 5A, MIR22HG inhibited growth and colony formation of SK-Hep-1, while miR10a-5p abrogated the inhibitory effects of MIR22HG. Similarly, miR10a-5p also reversed the inhibitory effects of MIR22HG on migration and invasion of liver cancer cells (Figure 5C). Consistent with these results, miR10a-5p inhibitor could reverse the promotion of MIR22HG knockdown on growth, migration and invasion of liver cancer cells (Figure S3A-C). Because NCOR2 was identified as a target downstream MIR22HG/miR10a-5p axis, we next investigated whether MIR22HG regulates HCC cell growth, migration and invasion through NCOR2. The results showed that MIR22HG overexpression suppressed cell growth, migration and invasion, while knockdown NCOR2 could partially reverse these effects (Figure 5D-F). In agreement with these results,

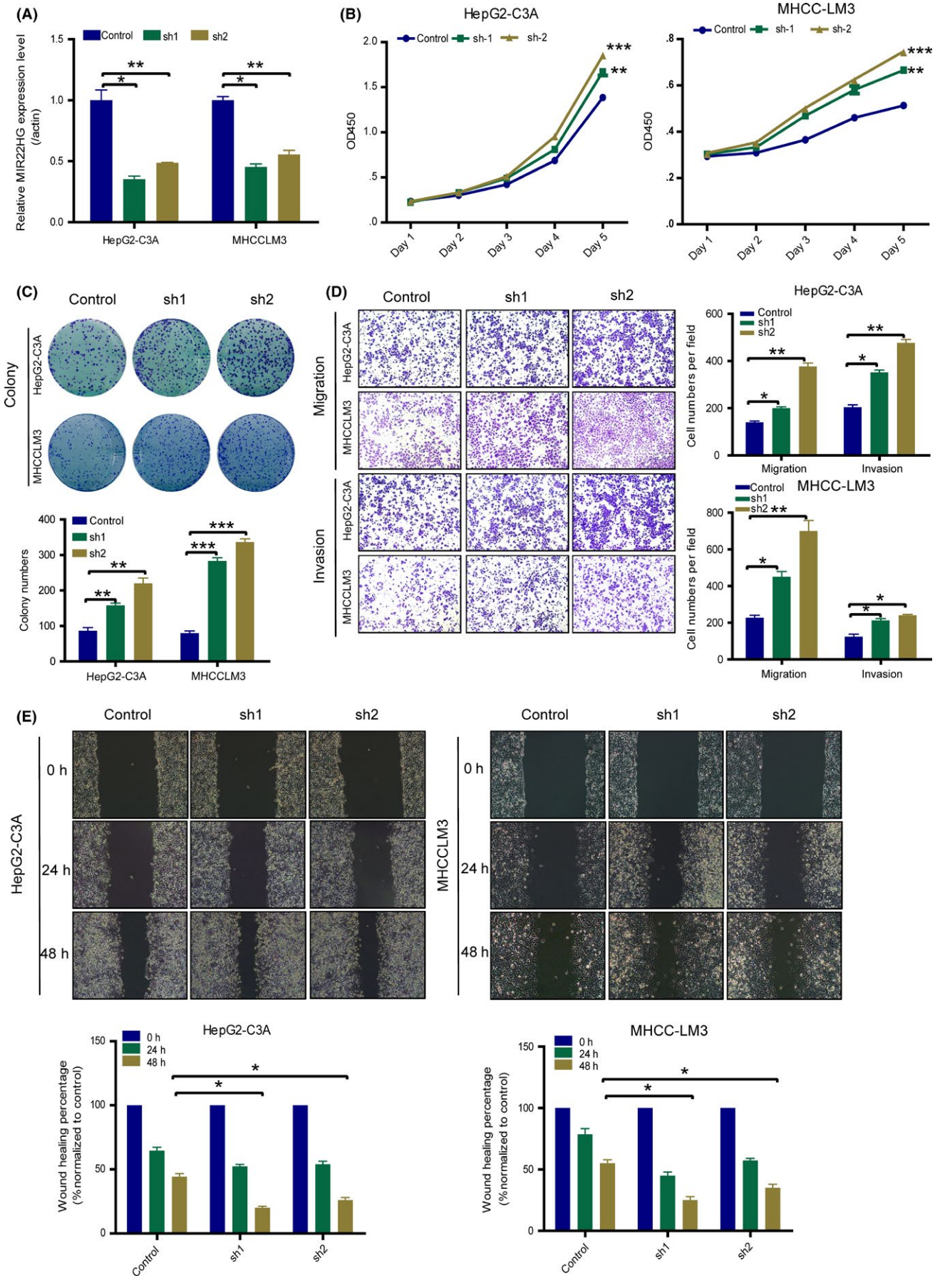
(A)
Relative MIR22HG expression level (/actin)
Control
sh1
sh2
HepG2-C3A
MHCCLM3
(B)
HepG2-C3A
MHCC-LM3
Control
sh-1
sh-2
OD450
Day 1
Day 2
Day 3
Day 4
Day 5
(C)
Control
sh1
sh2
Colony
HepG2-C3A
MHCCLM3
Colony numbers
(D)
Migration
Invasion
Cell numbers per field
Migration
Invasion
(E)
0 h
24 h
48 h
Wound healing percentage (%normalized to control)

FIGURE 2 MIR22HG knockdown promoted hepatocellular carcinoma (HCC) cell growth, migration and invasion. A, The level of MIR22HG in HepG2-C3A and MHCCLM3 cells after transfection with shMIR22HG or control was determined by quantitative PCR. B, Cell Counting Kit-8 (CCK-8) assays showed that MIR22HG knockdown promoted HCC growth. C, Colony formation assays showed that MIR22HG knockdown promoted HCC cell growth. D, Transwell assays showed that MIR22HG knockdown promoted migration and invasion of HCC cells. Results were expressed as cell numbers per field. E, Wound-healing assay showed that MIR22HG knockdown resulted in a faster closing of scratch wound. Results were expressed as wound healing percentage normalized to control. The error bars in all graphs represented SEM, and each experiment was repeated at least 3 times. $^{*}P < .05$, $^{**}P < .01$ and $^{***}P < .001$. Control, negative control

overexpression of NCOR2 could partly weaken the promotion of growth, migration and invasion induced by MIR22HG knockdown (Figure S3D-F). Overall, these results suggested that MIR22HG regulates HCC cell growth, migration and invasion by regulating the miR10a-5p/NCOR2 axis.

3.6 | MIR22HG regulates epithelial-mesenchymal transition through the miR10a-5p/NCOR2/Wnt/β-catenin pathway

NCOR2 is a nuclear receptor co-repressor that mediates transcriptional silencing of certain target genes.[18] It has been reported that NCOR2 depletion increases the invasive capacity of HCC cells. Mechanistically, NCOR2 promotes the association of NCOR2/NCOR2 with TBL1/TBLR1 and disrupts the binding of β-catenin to TBL1/TBLR1 complex, thereby inactivating the Wnt/β-catenin pathway.[19–21] Hence, we speculated that MIR22HG might inhibit HCC progression by upregulating NCOR2 and inactivating the Wnt/β-catenin pathway. To investigate this conjecture, we took advantage of TOP/FOP luciferase reporter assays to investigate the activation of the Wnt/β-catenin pathway. We found that knockdown of MIR22HG significantly increased the TOP/FOP activity, while restoring NCOR2 expression could reverse TOP/FOP upregulation induced by MIR22HG knockdown (Figure 6A). In agreement with this result, MIR22HG overexpression inhibited TOP/FOP activity and NCOR2 knockdown significantly rescued the inhibitory effect on TOP/FOP activity caused by MIR22HG overexpression (Figure 6A). These results demonstrated that MIR22HG regulates Wnt/β-catenin pathway through manipulating NCOR2 expression.

Metastasis is an important characteristic of cancer and is the leading cause of death for approximately 90% of cancer patients. Complicated signaling pathways are involved in tumor metastasis. Among them, epithelial-mesenchymal transition (EMT) is a major pathway affecting metastasis.[22–25] Previous studies indicated that Wnt/β-catenin pathway plays an important role in the EMT of cancer cells.[26,27] Hence, we speculated that MIR22HG might inhibit EMT by inactivating the Wnt/β-catenin pathway. We detected the EMT markers following MIR22HG overexpression or knockdown. Western blot analysis showed that MIR22HG knockdown increased mesenchymal markers N-cadherin and vimentin, and decreased epithelial marker E-cadherin, while these effects could be partially restored by miR10a-5p inhibitor (Figure 6B). Moreover, overexpressing MIR22HG induced expression of epithelial markers and reduced expression of mesenchymal markers. These effects could be partially restored by miR10a-5p mimic. Consistent with western blot analysis, immunofluorescence experiment staining of vimentin also suggested similar results (Figure 6C). All these results demonstrated that MIR22HG regulated HCC EMT by competitively binding miR10a-5p and inactivating Wnt/β-catenin pathway (Figure 6D).

4 | DISCUSSION

In recent years, emerging research has revealed that lncRNA play an important role in HCC progression. Li et al[28] found that LINC01138 frequently amplified in HCC promoted cell proliferation and invasion by physically interacting with PRMT5. Zhang et al[29] showed that lncRNA TSLNC8 acted as a tumor suppressor that inactivates the interleukin-6/STAT3 signaling pathway. Jiang et al[30] found that lnc-EGFR promotes HCC growth by stimulating T regulatory cell differentiation, thus promoting hepatocellular carcinoma immune evasion. In this study, we found that MIR22HG suppressed growth, migration and invasion of HCC cells. MIR22HG is located on chromosome 17p13.3, which is deleted with high frequency in cancers. Consistent with this finding, we found that MIR22HG transcript was significantly decreased in the HCC tissues, and low MIR22HG level was related to shorter overall survival (OS) and worse disease-free survival. Moreover, MIR22HG was negatively correlated with AFP ($P = .012$). Recent studies have shown that AFP is not just a biomarker for HCC but also an ardent promoter of liver cancer growth and progression.[31,32] We used a combination of AFP and MIR22HG level to predict the prognosis of liver cancer patients. First, ROC curve analysis showed that AFP + MIR22HG could more efficiently predict the prognosis of liver cancer patients (Figure S4A). At the same time, after univariate Cox proportional hazards regression analysis, AFP + MIR22HG was found to be more significantly correlated with the OS of HCC patients ($P = .015$) (Figure S4B). It turns out that combination with AFP + MIR22HG has a better prediction efficiency. These results indicated that MIR22HG may serve as a potential diagnostic and prognostic biomarker to improve HCC patients' outcome. Moreover, MIR22HG inhibited HCC growth, migration and invasion, suggesting that MIR22HG might act as a tumor suppressor in HCC.

One major molecular mechanism of lncRNA is acting as a molecular sponge for miRNA. In this study, combining bioinformatic analyses and luciferase reporter assays, we demonstrated that MIR22HG directly binds to miR10a-5p and inhibits miR10a-5p expression. Previous studies showed that miR10a-5p could play an important role in neoplasms. For example, Liu et al[15] found that

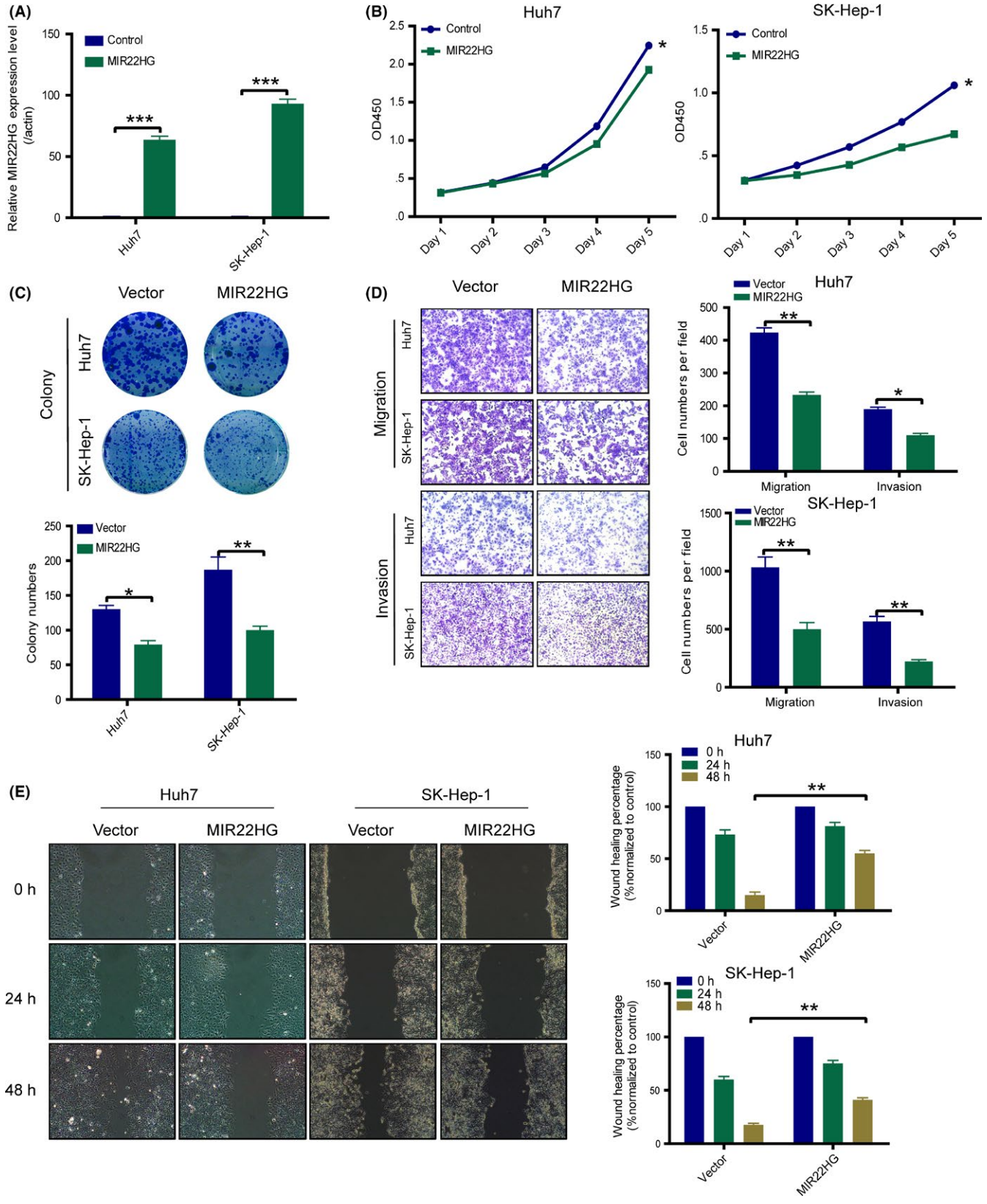

FIGURE 3 Overexpression of MIR22HG suppressed hepatocellular carcinoma (HCC) cell growth, migration and invasion. A, Quantitative PCR analysis of MIR22HG expression after MIR22HG overexpression. B, CCK8 assays and colony formation assays showed that MIR22HG overexpression inhibited liver cancer cells growth. C-E, Transwell and wound healing assays showed that MIR22HG overexpression inhibited migration and invasion of liver cancer cells. The error bars in all graphs represented SEM, and each experiment was repeated at least 3 times. *$P < .05$, **$P < .01$ and ***$P < .001$. Vector, empty vector

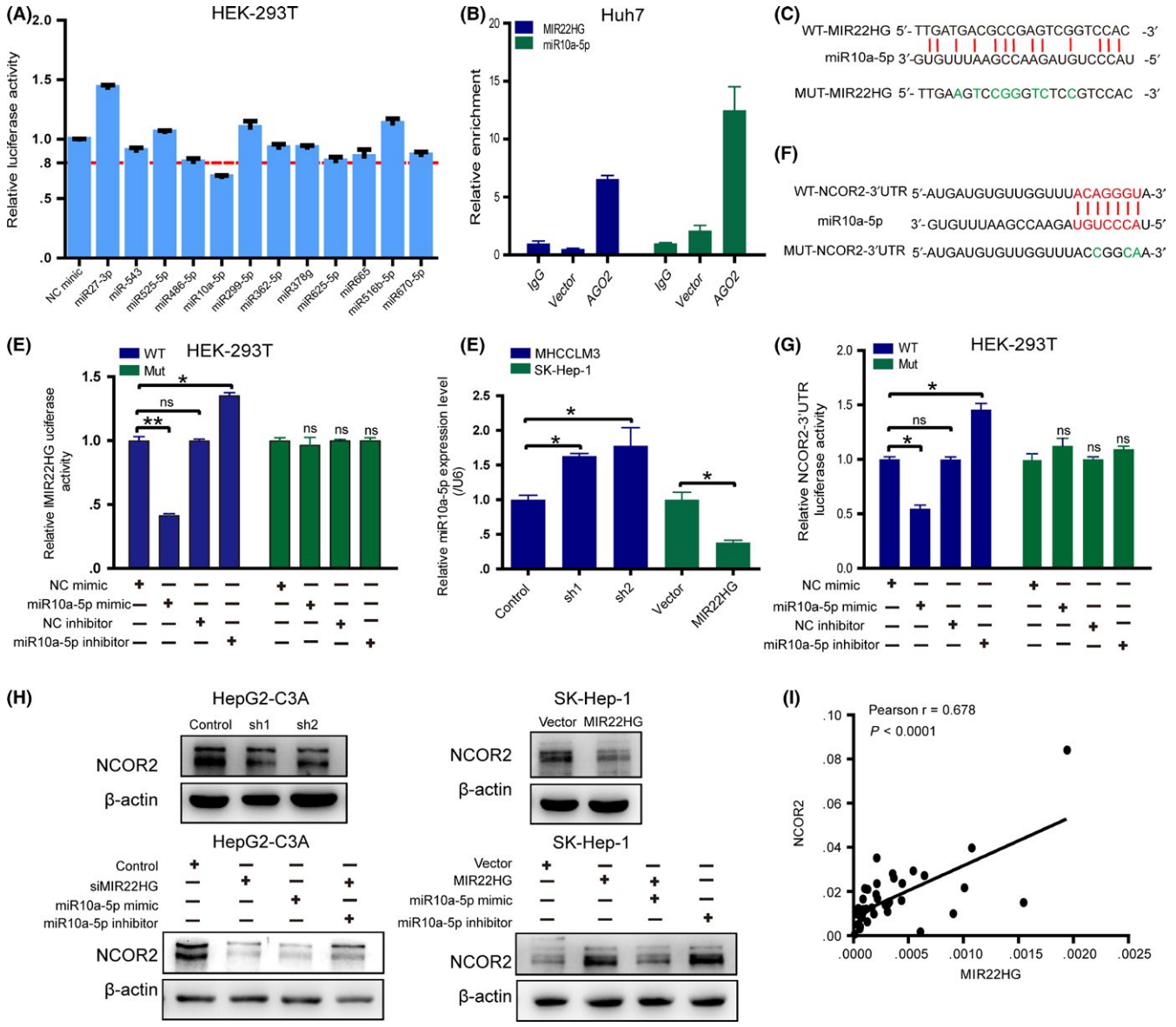

FIGURE 4 MIR22HG acts as a competing endogenous RNA and regulates NCOR2 expression by competitively binding miR10a-5p. A, 13 microRNA mimics transfected with psicheck2-MIR22HG plasmids into HEK-293T cells, respectively. miR10a-5p mimic can reduce the luciferase activity of MIR22HG. B, RIP assay indicated that both MIR22HG and miR10a-5p were significantly enriched in Ago2 immunoprecipitate. Empty vector was used as a nonspecific control. IgG acted as an internal control. C, Bioinformatics prediction of miR10a-5p binding sites in MIR22HG sequence using miRbase. D, Relative luciferase activities of wild-type (WT) and mutated (MUT) MIR22HG reporter plasmid in HEK-293T cells co-transfected with miR10a-5p mimic or inhibitor. E, miR10a-5p expression was determined by quantitative RT-PCR after MIR22HG overexpression or knockdown. F, Bioinformatics prediction of miR10a-5p binding sites in NCOR2 3′UTR sequence using miRbase. G, Relative luciferase activities of wild-type (WT) and mutated (MUT) NCOR2 3′UTR reporter plasmid in HEK-293T cells co-transfected with miR10a-5p mimic or inhibitor. H, Western blot detected NCOR2 protein levels after MIR22HG or miR10a-5p manipulation as indicated in the figure. I, Pearson's correlation analysis of the relationship between MIR22HG and NCOR2 mRNA expression levels in liver cancer tissues. The error bars in all graphs represent SEM, and each experiment was repeated at least 3 times. $^{*}P < .05$, $^{**}P < .01$ and $^{***}P < .001$

miR10a can promote human glioma cell migration by targeting PTEN. Zeng et al[16] showed that miR10a enhanced the metastatic potential of cervical cancer cells by targeting PTEN. Foley NH et al[14] concluded that miR-10a/b played major roles in the process of neural cell differentiation through direct targeting of NCOR2. In addition, miR-10a was reported to suppress colorectal cancer metastasis by targeting MMP14 and ACTG1.[13] These studies suggest that miR-10a can act as an oncogene or tumor suppressor according to content difference in cancers. However, the role of miR-10a in HCC remains unclear. Our study provides the first evidence that miR10a-5p promotes liver cancer cell growth, migration and invasion of HCC cells. Furthermore, miR10a is inversely correlated with MIR22HG in liver cancer tissues. Overexpression of miR10a-5p reverses the anti–metastatic ability of MIR22HG.

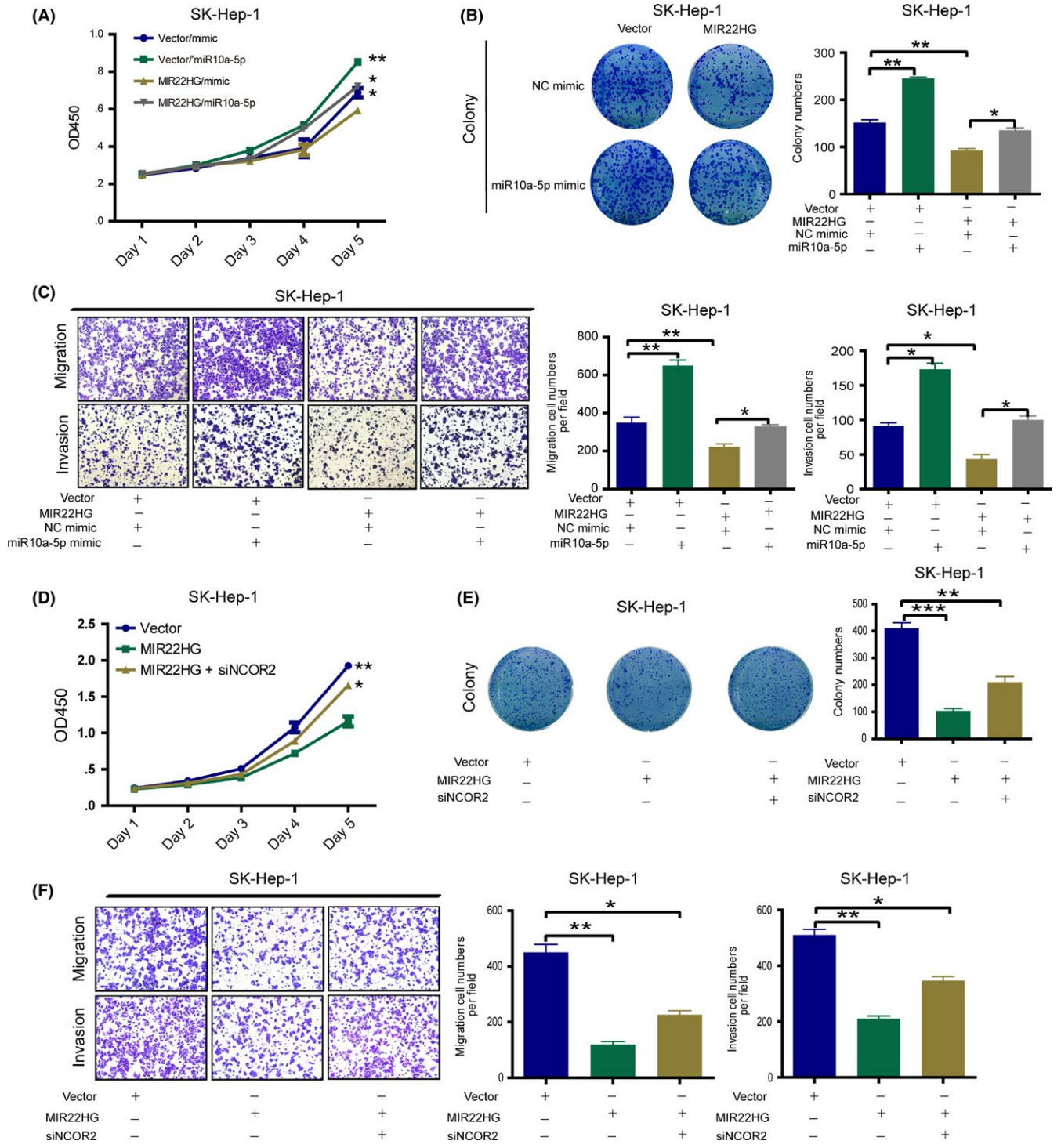

FIGURE 5 MIR22HG inhibited hepatocellular carcinoma (HCC) cell growth, migration and invasion by inhibiting the miR10a-5p/NCOR2 axis. A-C, miR10a-5p partially reversed the effects of MIR22HG on the growth, migration and invasion of liver cancer cells. D-F, NCOR2 partially restored the effects of MIR22HG on the growth, migration and invasion of liver cancer cells. The error bars in all graphs represented SEM, and each experiment was repeated at least 3 times. $^{*}P < .05$, $^{**}P < .01$ and $^{***}P < .001$

These results indicated that miR10a-5p could act as a downstream target of MIR22HG in liver cancer cells.

We further explore the downstream signaling pathway of miR10a-5p in HCC. Through bioinformatic analyses, qPCR, luciferase reporter assays and western blot analysis, we demonstrated that NCOR2 was the target of miR10a-5p in liver cancer cells. NCOR2, nuclear receptor corepressor 2 (also known as SMRT), mediates liver cancer cells of certain target genes.[18,20] Chao Qu et al[20] have shown that NCOR2 can bind with TBL1/TBLR1, which disrupts the binding of β-catenin to TBL1/TBLR1 complex, thereby inactivating the

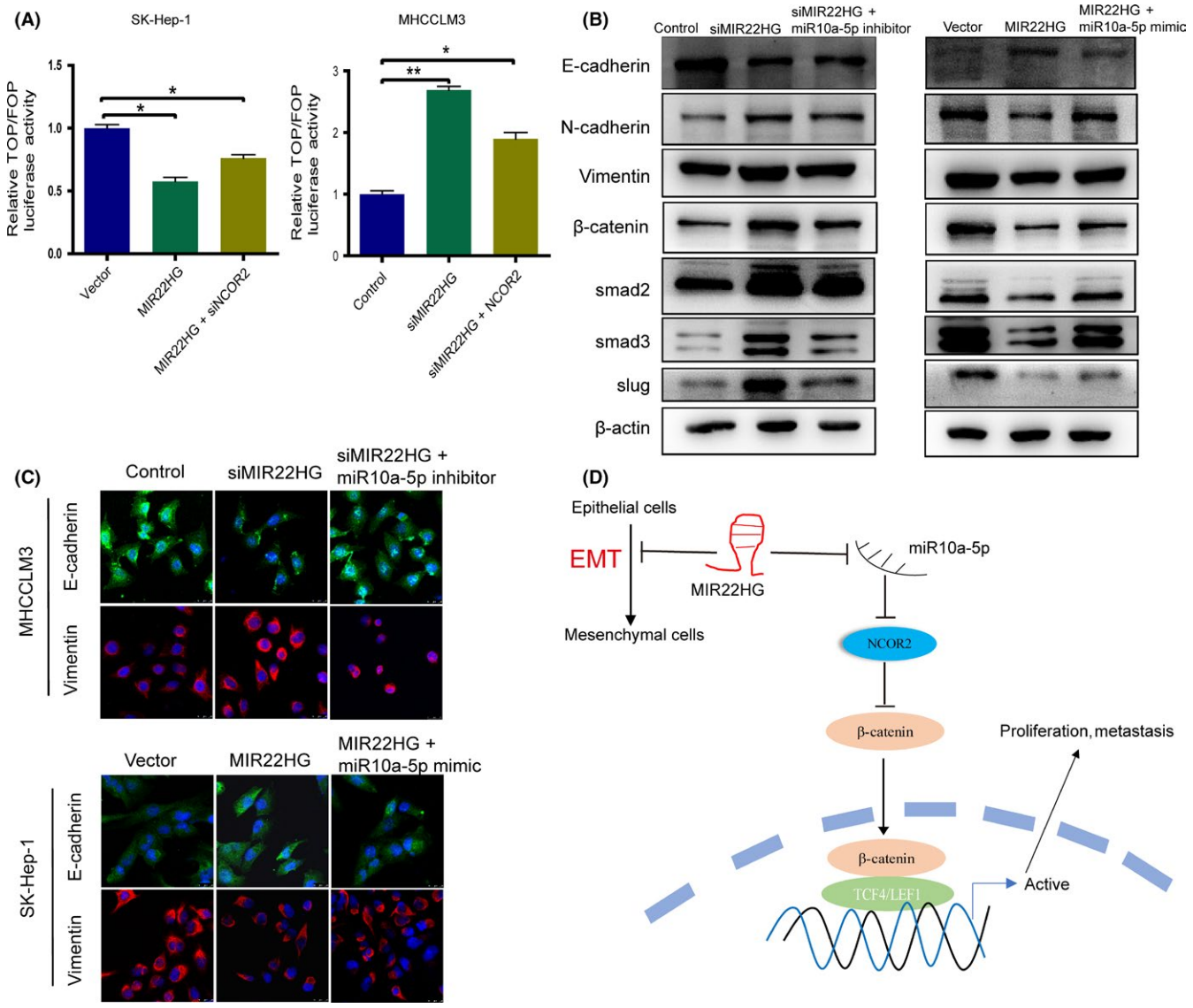

FIGURE 6 MIR22HG inhibited epithelial-mesenchymal transition (EMT) by competitively binding miR10a-5p and activating the Wnt/β-catenin pathway. A, Dual-luciferase assay showed that MIR22HG and NCOR2 inhibited TOP/FOP reporter activity in SK-Hep1 and MHCCLM3 cells. B, Western blot assays were used to analyze EMT marker expression after MIR22HG overexpression or knockdown with/without miR10a-5p mimic and inhibitor transfection. C, Immunofluorescence assays determined the vimentin level upon MIR22HG overexpression or knockdown with/without miR10a-5p mimic and inhibitor transfection. D, A schematic model depicting the molecular mechanism of MIR22HG in hepatocellular carcinoma (HCC)

Wnt/β-catenin pathway. Here, we also found that overexpression of NCOR2 significantly decreased TOP/FOP activity, indicating that the Wnt/β-catenin pathway was inhibited by NCOR2 in HCC cells. Interestingly, MIR22HG also inhibited TOP/FOP activity and the inhibitory effect could be reversed by NCOR2 knockdown. Previous studies have indicated that Wnt/β-catenin pathway plays an important role in cancer EMT, and many lncRNA have been demonstrated to modulate tumor EMT by targeting the key components of the Wnt/β-catenin pathway. We also demonstrated that MIR22HG regulated the Wnt/β-catenin signaling pathway by targeting NCOR2, and knockdown of MIR22HG increased epithelial markers but decreased mesenchymal markers. These data demonstrated that MIR22HG suppressed EMT by modulating the Wnt/β-catenin pathway.

In conclusion, we explored a new mechanism of lncRNA MIR22HG in HCC. MIR22HG worked as a tumor suppressor that inhibited the tumorigenesis and progression of HCC through the MIR22HG/miR10a-5p/NCOR2 axis, and is a potential therapeutic target for HCC.

CONFLICT OF INTEREST

The authors declare that they have no conflict of interest.

ORCID

Linhui Liang https://orcid.org/0000-0002-1284-138X

REFERENCES

1. Bray F, Ferlay J, Soerjomataram I, Siegel RL, Torre LA, Jemal A. Global cancer statistics 2018: GLOBOCAN estimates of incidence and mortality worldwide for 36 cancers in 185 countries. *CA Cancer J Clin*. 2018;00:1-31.
2. Visvader JE. Cells of origin in cancer. *Nature*. 2011;469:314-322.
3. Bruix J, Gores GJ, Mazzaferro V. Hepatocellular carcinoma: clinical frontiers and perspectives. *Gut*. 2014;63:844-855.
4. Mercer TR, Dinger ME, Mattick JS. Long non-coding RNAs: insights into functions. *Nat Rev Genet*. 2009;10:155-159.
5. Geisler S, Coller J. RNA in unexpected places: long non-coding RNA functions in diverse cellular contexts. *Nat Rev Mol Cell Bio*. 2013;14:699-712.
6. Salmena L, Poliseno L, Tay Y, Kats L, Pandolfi PP. A ceRNA hypothesis: The Rosetta Stone of a hidden RNA language? *Cell*. 2011;146:353-358.
7. Karreth FA, Tay Y, Perna D, et al. *In vivo* identification of tumor-suppressive PTEN ceRNAs in an oncogenic BRAF-induced mouse model of melanoma. *Cell*. 2011;147:382-395.
8. Gong C, Maquat LE. lncRNAs transactivate STAU1-mediated mRNA decay by duplexing with 3′ UTRs via Alu elements. *Nature*. 2011;470:284-288.
9. Zhang D, Zou X, Cao C, et al. Identification and functional characterization of long non-coding RNAMIR22HG as a tumor suppressor for hepatocellular carcinoma. *Theranostics*. 2018;8:3751-3765.
10. Dong Y, Yan W, Zhang SL, et al. Prognostic values of long non-coding RNA MIR22HG for patients with hepatocellular carcinoma after hepatectomy. *Oncotarget*. 2017;8:114041-114049.
11. Su W, Feng S, Chen X, et al. Silencing of long non-coding RNA MIR22HG triggers cell survival/death signaling via oncogenes YBX1, MET, and p21 in lung cancer. *Cancer Res*. 2018;78:222-2018.
12. Cui Z, An X, Li J, Liu Q, Liu W. LncRNA MIR22HG negatively regulates miR-141-3p to enhance DAPK1 expression and inhibits endometrial carcinoma cells proliferation. *Biomed Pharmacother*. 2018;104:223-228.
13. Liu Y, Zhang Y, Wu H, et al. miR-10a suppresses colorectal cancer metastasis by modulating the epithelial-to-mesenchymal transition and anoikis. *Cell Death Dis*. 2017;8:e2739.
14. Foley NH, Bray I, Watters KM, et al. MicroRNAs 10a and 10b are potent inducers of neuroblastoma cell differentiation through targeting of nuclear receptor corepressor 2. *Cell Death Differ*. 2011;18:1089-1098.
15. Liu S, Sun J, Lan Q. TGF-beta-induced miR10a/b expression promotes human glioma cell migration by targeting PTEN. *Mol Med Rep*. 2013;8:1741-1746.
16. Zeng T, Li G. MicroRNA10a enhances the metastatic potential of cervical cancer cells by targeting phosphatase and tensin homologue. *Mol Med Rep*. 2014;10:1377-1382.
17. Khan S, Wall D, Curran C, Newell J, Kerin MJ, Dwyer RM. MicroRNA-10a is reduced in breast cancer and regulated in part through retinoic acid. *BMC Cancer*. 2015;15:345.
18. Mottis A, Mouchiroud L, Auwerx J. Emerging roles of the corepressors NCoR1 and SMRT in homeostasis. *Gene Dev*. 2013;27:819-835.
19. Choi HK, Choi KC, Yoo JY, et al. Reversible SUMOylation of TBL1-TBLR1 regulates beta-catenin-mediated Wnt signaling. *Mol Cell*. 2011;43:203-216.
20. Qu C, He D, Lu X, et al. Salt-inducible Kinase (SIK1) regulates HCC progression and WNT/beta-catenin activation. *J Hepatol*. 2016;64:1076-1089.
21. Oberoi J, Fairall L, Watson PJ, et al. Structural basis for the assembly of the SMRT/NCoR core transcriptional repression machinery. *Nat Struct Mol Biol*. 2011;18:177-184.
22. Han S, Hwang HS, Chae JS, et al. CIIA induces the epithelial–mesenchymal transition and cell invasion. *Biochem Bioph Res Co*. 2009;387:548-552.
23. Craene BD, Berx G. Regulatory networks defining EMT during cancer initiation and progression. *Nat Rev Cancer*. 2013;13:97-110.
24. Thiery JP, Acloque H, Huang RYJ, Nieto MA. Epithelial-mesenchymal transitions in development and disease. *Cell*. 2009;139:871-890.
25. Brabletz T, Kalluri R, Nieto MA, Weinberg RA. EMT in cancer. *Nat Rev Cancer*. 2018;18:128-134.
26. Ma F, Li W, Liu C, et al. MiR-23a promotes TGF-beta1-induced EMT and tumor metastasis in breast cancer cells by directly targeting CDH1 and activating Wnt/beta-catenin signaling. *Oncotarget*. 2017;8:69538-69550.
27. Qi J, Yu Y, Akilli Öztürk Ö, et al. New Wnt/β-catenin target genes promote experimental metastasis and migration of colorectal cancer cells through different signals. *Gut*. 2016;65:1690-1701.
28. Li Z, Zhang J, Liu X, et al. The LINC01138 drives malignancies via activating arginine methyltransferase 5 in hepatocellular carcinoma. *Nat Commun*. 2018;9:1514-1572.
29. Zhang J, Li Z, Liu L, et al. Long noncoding RNA TSLNC8 is a tumor suppressor that inactivates the interleukin-6/STAT3 signaling pathway. *Hepatology*. 2018;67:171-187.
30. Jiang R, Tang J, Chen Y, et al. The long noncoding RNA lnc-EGFR stimulates T-regulatory cells differentiation thus promoting hepatocellular carcinoma immune evasion. *Nat Commun*. 2017;8:15129.
31. Yamashita T, Forgues M, Wang W, et al. EpCAM and -fetoprotein expression defines novel prognostic subtypes of hepatocellular carcinoma. *Cancer Res*. 2008;68:1451-1461.
32. Kimura H, Ohkawa K, Miyazaki M, et al. Subclassification of patients with intermediate-stage (Barcelona Clinic Liver Cancer stage-B) hepatocellular carcinoma using the up-to-seven criteria and serum tumor markers. *Hepatol Int*. 2017;11:105-114.
33. Mizejewski GJ. Does alpha-fetoprotein contribute to the mortality and morbidity of human hepatocellular carcinoma? A commentary. *J Hepatocell Carcinoma*. 2016;3:37-40.

SUPPORTING INFORMATION

Additional supporting information may be found online in the Supporting Information section at the end of the article.

How to cite this article: Wu Y, Zhou Y, Huan L, et al. LncRNA MIR22HG inhibits growth, migration and invasion through regulating the miR-10a-5p/NCOR2 axis in hepatocellular carcinoma cells. *Cancer Sci*. 2019;110:973–984. https://doi.org/10.1111/cas.13950